═══REVIEW COMMONS MANUSCRIPT═══

IMPORTANT:

- Manuscripts submitted to Review Commons are peer reviewed in a journal-agnostic way.
- Upon transfer of the peer reviewed preprint to a journal, the referee reports will be available in full to the handling editor.
- The identity of the referees will NOT be communicated to the authors unless the reviewers choose to sign their report.
- The identity of the referee will be confidentially disclosed to any affiliate journals to which the manuscript is transferred.

GUIDELINES:

- For reviewers: https://www.reviewcommons.org/reviewers
- For authors: https://www.reviewcommons.org/authors

CONTACT:

The Review Commons office can be contacted directly at: office@reviewcommons.org

GPLD1 functions as a scavenger chaperone mediating lysosomal degradation of extracellular aberrant proteins

Mizuki Tsuchiya[1], Akira Matsuura[2], Eisuke Itakura[2*]

[1] Department of Biology, Graduate school of Science and Engineering, Chiba University, Chiba, Japan

[2] Department of Biology, Graduate School of Science, Chiba University. Chiba, Japan

Abstract

Loss of proteostasis leads to the accumulation of aberrant proteins, including aggregated proteins and amyloid fibrils, which contribute to various diseases. Protein quality control systems are essential for maintaining proteostasis by removing these aberrant proteins. Although intracellular protein quality control mechanisms are well characterized, the pathways responsible for degradation of aberrant proteins outside the cell remain poorly understood. We previously identified the chaperone- and receptor-mediated extracellular protein degradation (CRED) pathway, in which the extracellular chaperone clusterin binds misfolded proteins and the resulting clusterin–aberrant protein complex is delivered to lysosomes via endocytosis, thereby clearing extracellular aberrant proteins. However, it remains unclear whether other chaperones are involved in the CRED pathway.

To identify novel extracellular chaperones, plasma factors that bind serum amyloid A1 (SAA1) were investigated. Glycosylphosphatidylinositol-specific phospholipase D1 (GPLD1) was found to directly bind SAA1 in vitro and promote lysosomal degradation of SAA1 in cultured cells. This activity was independent of GPLD1's cleavage activity for GPI-anchored proteins. Furthermore, we found that GPLD1 mediates lysosomal degradation of misfolded proteins, with cell surface heparan sulfate acting as a receptor for GPLD1. Our data demonstrate that GPLD1 is a novel scavenger chaperone with substrate specificity distinct from clusterin, responsible for degrading extracellular aberrant proteins.

Keywords

Protein quality control system, Proteostasis, Lysosome, Aberrant protein, Protein degradation, Extracellular chaperone

Introduction

The accumulation of aberrant proteins leads to the formation of aggregates, which underlies the pathogenesis of various neurodegenerative diseases (Hipp *et al*, 2019; Tyedmers *et al*, 2010). For instance, amyloid fibrils, composed of β-sheet-rich proteins, deposit in tissues and cause a condition known as amyloidosis (Sawaya *et al*, 2021). To maintain proteostasis, cells rely on intracellular protein quality control systems, including autophagy and the ubiquitin-proteasome system, which degrade misfolded or damaged proteins (Klionsky *et al*, 2021; Wolff *et al*, 2014). The cytoplasm is densely populated with proteins, reaching concentrations of approximately 200–300 g/L. Similarly, extracellular compartments, such as the bloodstream, also exhibit high protein concentrations at approximately 80 g/L (Ellis, 2001). Although intracellular protein quality control mechanisms are well-characterized (Rusilowicz-Jones *et al*, 2022), the pathways responsible for the clearance of aberrant proteins in the extracellular environment remain poorly understood (Wyatt *et al*, 2013). In our previous study, we identified a novel pathway termed chaperone-mediated extracellular protein degradation (CRED) (Itakura *et al*, 2020). In this pathway, the extracellular chaperone clusterin recognizes and binds misfolded proteins, forming a complex that is subsequently internalized and selectively degraded in lysosomes via the cell surface heparan sulfate (HS) receptor. Clusterin also facilitates lysosomal degradation of amyloid β, a prototypical amyloidogenic protein (Calero *et al*, 2000; Itakura *et al.*, 2020). This mechanism contributes to the clearance of misfolded proteins from the extracellular environment (Itakura *et al.*, 2020). We have also found that α2-macroglobulin facilitates lysosomal degradation of extracellular aberrant proteins (Tomihari *et al*, 2023). However, the involvement of additional chaperones in the CRED pathway remains incompletely understood. In the present study, we investigated the existence of a novel CRED factor responsible for the degradation of extracellular amyloidogenic proteins. Amyloidosis is a pathological condition characterized by the extracellular deposition of insoluble, fibrillar proteins (amyloid fibrils), which leads to progressive organ dysfunction (Louros *et al*, 2023). In humans, more than 30 proteins have been identified as precursors of amyloid fibrils (Sipe *et al*, 2016). Serum amyloid A (SAA) is one such protein, strongly associated with amyloidosis and often arising as a complication of chronic inflammatory diseases. These conditions are marked by the deposition of insoluble amyloid fibrils in affected organs and tissues (Sun & Ye, 2016). AA amyloidosis specifically results from prolonged inflammation, which drives sustained overproduction of SAA1. This overproduction ultimately leads to the aggregation and deposition of AA amyloid in tissues (Gaffney, 2017). Human SAA1 is encoded by one of four SAA genes. Among these, SAA1 and SAA2 are acute-phase genes that are transcriptionally upregulated in response to inflammatory cytokines, which are induced by infections or autoimmune diseases. These proteins play roles in modulating cytokine synthesis and neutrophil chemotaxis (Uhlar & Whitehead, 1999). Consequently, identifying mechanisms responsible for the degradation of SAA1 in the bloodstream is of critical importance for prevention and mitigation of amyloidosis and related inflammatory conditions. Glycosylphosphatidylinositol-specific phospholipase D1 (GPLD1) is a secreted protein of approximately 110 kDa, predominantly produced by the liver (LeBoeuf *et al*, 1998). It possesses a catalytic site that cleaves the lipid-binding domain of glycosylphosphatidylinositol (GPI)-anchored proteins, which are exposed on the extracellular surface of the cell membrane. This enzymatic activity facilitates the release of GPI-anchored

proteins from the cell surface (Cao *et al*, 2023). Recent studies have shown that plasma levels of GPLD1 increase following physical exercise (Horowitz *et al*, 2020; Ren *et al*, 2024). Moreover, the exogenous expression of GPLD1 in aged mice has been reported to enhance cognitive function (Horowitz *et al.*, 2020). In this study, we identified GPLD1 as a plasma factor that binds SAA1, using mass spectrometry-based analysis. By developing an internalization assay using fluorescently tagged GPLD1, we demonstrated that GPLD1 promotes lysosomal degradation of SAA1 and other misfolded proteins. Mechanistically, HS functions as a cell surface receptor that mediates internalization of the GPLD1–aberrant protein complex. Notably, GPLD1 exhibited greater internalization activity toward SAA1 than clusterin, suggesting that SAA1 is a physiological substrate of GPLD1. These findings indicate that GPLD1 possesses distinct substrate specificity compared to the known extracellular chaperone clusterin and functions as a novel scavenger chaperone involved in the clearance of extracellular aberrant proteins.

Results

GPLD1 binds SAA1 in plasma proteins

To identify a novel extracellular chaperone, we analyzed SAA1-binding proteins from bovine plasma, which is rich in extracellular proteins, using His-ALFA-tagged SAA1 (ALFA-SAA1) as bait. Given the amyloidogenic nature of SAA1, ALFA-SAA1 was purified from *Escherichia coli* under denaturing conditions in the presence of urea. The purified ALFA-SAA1 protein was then incubated with bovine plasma and subjected to immunoprecipitation using ALFA nanobody-conjugated beads. Ruby staining revealed a range of proteins bound to ALFA-SAA1 (Fig. 1A), and these were subsequently identified by mass spectrometry (Table S1). Notably, clusterin and apolipoprotein E—both known to interact with extracellular aberrant proteins—were among the identified proteins (Mahley *et al*, 2009; Matsubara *et al*, 1996), suggesting that this dataset may contain previously unrecognized extracellular chaperones involved in proteostasis. After excluding well-characterized proteins, we shortlisted seven candidate proteins as potential extracellular chaperones. We then examined whether these candidates were internalized in cells in an SAA1-dependent manner and subsequently degraded in lysosomes. To detect lysosomal uptake of the candidate chaperones, we developed an internalization assay employing tandem-tagged constructs comprising red fluorescent protein (RFP:mCherry), green fluorescent protein (GFP:sfGFP), and a His-tag. RFP is highly resistant to lysosomal proteases and acidic pH, whereas GFP is more susceptible to degradation. Therefore, upon internalization and trafficking of RFP-GFP-His-tagged chaperone candidates into lysosomes, only the RFP portion accumulates, whereas the GFP signal is lost (Fig. 1B). The RFP-GFP-His (RG)-tagged candidate proteins were overexpressed in Flp-In T-REx HEK293 cells. The conditioned medium containing RG-tagged fusion proteins was collected and purified using His-tag affinity chromatography. For the internalization assay, ALFA-SAA1 was mixed with serum-free medium containing the RG-tagged fusion protein and incubated at 37 °C for 2 h before being added to cultured cells. After 18 h of incubation, the cells were harvested, and GFP and RFP fluorescence intensities were measured using flow cytometry. The internalization assay revealed that one candidate, GPLD1-RG, exhibited an SAA1-dependent increase in RFP fluorescence intensity (Fig. 1C). To confirm whether GPLD1-RG underwent lysosomal degradation, cells were treated with medium containing GPLD1-RG in the presence or absence of bafilomycin A_1 (BafA), an inhibitor of lysosomal acidification and partial endocytosis (Baravalle *et al*, 2005). BafA treatment suppressed the SAA1-dependent increase in RFP accumulation, whereas GFP intensity increased (Fig. 1D), suggesting inhibition of lysosomal degradation. We further verified the lysosomal degradation of GPLD1-RG biochemically using an RFP cleavage assay (Tomihari *et al*, 2021). This assay detects the release of free 25-kDa RFP fragments generated from lysosomal digestion of the 160-kDa GPLD1-RG fusion protein. Free RFP was detected in cells treated with GPLD1-RG (Fig. 1E), and the amount of free RFP increased in the presence of SAA1. Notably, this increase was attenuated by BafA treatment. These results indicate that the GPLD1–SAA1 complex is internalized and subsequently degraded in lysosomes.

GPLD1 binds aberrant proteins

To investigate whether GPLD1 directly interacts with substrate proteins, we conducted

immunoprecipitation assays using recombinant proteins. ALFA-SAA1 was incubated with GPLD1-RG, followed by immunoprecipitation using ALFA nanobody-conjugated beads. GPLD1 was found to co-immunoprecipitate with ALFA-SAA1 (Fig. 2A). To assess binding in the context of protein misfolding, we employed luciferase as a model substrate as it undergoes heat-induced denaturation at 42°C (Glover & Lindquist, 1998; Rodrigo-Brenni *et al*, 2014). Immunoprecipitation revealed that the association between GPLD1-RG and luciferase was enhanced under conditions promoting misfolding (Fig. 2B). These findings demonstrate that GPLD1 directly binds aberrant and misfolded proteins.

GPLD1 and the aberrant protein complex is degraded by lysosomes

To investigate lysosomal degradation mediated by GPLD1, we conducted an internalization assay using serum-free medium containing GPLD1-RG and various substrate proteins. S-formylglutathione hydrolase (ESD), a substrate for the extracellular chaperones clusterin and α2-macroglobulin (α2M), has also been identified as a misfolded protein substrate (Tomihari *et al.*, 2023). GPLD1-RG was mixed with luciferase or ALFA-tagged ESD (ALFA-ESD) in serum-free medium. The luciferase mixture was denatured at 42°C for 30 min, whereas the ALFA-ESD mixture was denatured at 50°C for 1 h to induce misfolding. After replacing the cell culture medium with medium containing the GPLD1-RG–substrate mixtures, cells were incubated overnight and subsequently analyzed by flow cytometry. Compared to the GPLD1-RG–only controls, the addition of luciferase or ALFA-ESD significantly increased RFP intensity (Fig. 3A), suggesting that GPLD1-RG promotes lysosomal degradation of these misfolded proteins.

To examine the subcellular localization of GPLD1, we performed double immunostaining using a GPLD1 construct fused to Gamillus, a GFP resistant to lysosomal degradation (GPLD1-Gamillus-His) (Shinoda *et al*, 2018). Cells were treated as described in Fig. 1C and 3A with GPLD1-Gamillus, followed by immunostaining with an anti-LAMP1 antibody, a marker of the lysosomal membrane (Fig. 3B). In cells treated with GPLD1-Gamillus alone, green fluorescence was barely detectable. Conversely, the presence of luciferase or ALFA-SAA1 markedly increased both the number and intensity of green fluorescent puncta. These GPLD1-Gamillus puncta co-localized with LAMP1-positive red signals, indicating lysosomal localization. Treatment with bafA suppressed the accumulation of RFP, but not GFP, in cells treated with GPLD1-RG and luciferase (Fig. 3C). Additionally, an RFP cleavage assay demonstrated that bafA inhibited the increase of free RFP in cells exposed to GPLD1-RG and SAA1 (Fig. 3D). These combined cell biological and biochemical findings suggest that the GPLD1–aberrant protein complex is internalized and trafficked to the lysosomal lumen for degradation.

Vascular endothelial cells exhibit higher levels of internalization of GPLD1 complex

We performed GPLD1-RG internalization assays in four cell lines of distinct tissue origins: HepG2 (liver carcinoma), U2OS (osteosarcoma), T98G (glioblastoma), and HuEhT (immortalized human vascular endothelial cells). Although all cell lines showed increased internalization upon exposure to substrate proteins, the extent varied among them. HepG2 cells exhibited the lowest levels of

internalization, whereas HuEhT cells displayed the highest (Fig. S1). These findings suggest that the GPLD1–substrate complex is broadly internalized across diverse cell types, indicating its potential activity in a wide range of tissues.

Catalytic activity of GPLD1 is not required for internalization of the GPLD1 complex

GPLD1 exhibits catalytic activity that specifically hydrolyzes the inositol phosphate bond of GPI-anchored proteins on the cell membrane (Cao *et al.*, 2023). Mutations at His133 or His158 abolish this enzymatic activity (Raikwar *et al*, 2005). To determine whether GPLD1's catalytic function is required for substrate-dependent intracellular uptake, we generated two catalytically inactive mutants—GPLD1-H133N-RG and GPLD1-H158N-RG—by substituting histidine residues at positions 133 and 158 with asparagine. Internalization assays revealed that these mutants did not significantly reduce RFP accumulation compared to wild-type GPLD1 (Fig. 4A). Given that these mutations effectively eliminate enzymatic activity (Horowitz *et al.*, 2020), yet internalization still occurred, these findings indicate that GPLD1's catalytic activity is not essential for substrate-mediated uptake. To further investigate whether GPI-anchored proteins are involved in GPLD1 internalization, we generated GPAA1 knockout (KO) cells. GPAA1 is a critical GPI transamidase required for the synthesis of GPI-anchored proteins (Eisenhaber *et al*, 2014). Western blot analysis confirmed the absence of GPAA1 protein in KO cells (Fig. 4B), and trafficking of GFP-tagged GPI-anchored proteins to the plasma membrane was disrupted in these cells (Fig. 4C), confirming the loss of surface GPI-anchored proteins. Nevertheless, GPLD1 internalization was not impaired in GPAA1 KO cells (Fig. 4D), suggesting that uptake of the GPLD1–substrate complex occurs independently of GPI-anchored proteins.

Cell surface HS facilitates GPLD1 internalization

Nearly all vertebrate cells express a limited set of cell-surface HS proteoglycans, which serve as receptors for various growth factors and viruses (Liu & Thorp, 2002; Pillay *et al*, 2016; Xu & Esko, 2014; Yayon *et al*, 1991). In addition, HS functions as a membrane receptor for the substrate-dependent internalization of clusterin (Itakura *et al.*, 2020). To investigate whether HS is similarly involved in the substrate-dependent uptake of GPLD1, we first examined the potential direct interaction between GPLD1 and HS. A pulldown assay was performed using heparin-coated beads, which mimic the structure of HS chains. GPLD1-RG, but not the RG tag alone, was precipitated by the heparin-coated beads (Fig. 5A), indicating a specific interaction. Furthermore, this binding was competitively inhibited by the addition of free heparin.

We conducted GPLD1-RG internalization assays using EXT1 KO cells, which lack EXT1, an essential enzyme for the biosynthesis of HS (McCormick *et al*, 1998). In these cells, the luciferase-induced increase in RFP levels was reduced to less than half compared to wild-type cells and EXT1 overexpression (EXT1 OE) cells (Fig. 5B). Notably, overexpression of EXT1 in KO (EXT1 OE-EXT1 KO) cells restored RFP intensity, suggesting that HS biosynthesis is critical for GPLD1-RG internalization. To further examine the direct role of extracellular HS in this process, we performed a competitive inhibition assay using free heparin. GPLD1-RG was mixed with luciferase

or ALFA-SAA1 in serum-free medium and incubated with cells in the presence or absence of excess heparin. The addition of heparin significantly reduced GPLD1-RG internalization, lowering uptake to less than half of the original level (Fig. 5C). Collectively, these results indicate that cell-surface HS mediates substrate-dependent internalization of GPLD1.

Substrate selectivity of GPLD1 differs from that of clusterin

To compare the substrate selectivity of GPLD1 with that of clusterin, we performed internalization assays using clusterin-RG and GPLD1-RG at equal concentrations. Three types of substrate proteins were tested: luciferase, ALFA-SAA1, and amyloid β 1-42 (Aβ42)-ALFA. Clusterin-RG induced the highest increase in RFP intensity in the presence of Aβ42, whereas its response to SAA1 was comparatively lower. Conversely, GPLD1-RG showed a greater increase in RFP intensity with SAA1 than with Aβ42 (Fig. 6A). These results suggest that GPLD1 exhibits a substrate selectivity profile distinct from that of clusterin.

Discussion

We previously identified the CRED pathway, in which extracellular chaperones such as clusterin bind aberrant proteins, forming complexes that are selectively internalized via specific cell-surface receptors and subsequently degraded in lysosomes, thereby facilitating the removal of aberrant proteins from the extracellular space (Itakura *et al.*, 2020; Tomihari *et al.*, 2023). In the present study, we identified GPLD1 as a novel extracellular scavenger chaperone. Co-immunoprecipitation of purified GPLD1 demonstrated its ability to directly interact with SAA1 and misfolded proteins (Fig. 2). Internalization assays using GPLD1-RG showed that GPLD1 mediates the cellular uptake of both SAA1 and misfolded proteins (Fig. 3A). We further confirmed that this internalization leads to lysosomal degradation, as evidenced by fluorescence microscopy and RFP cleavage assays (Fig. 3B and 3C). Additionally, our data indicate that this process is dependent on cell-surface HS (Fig. 5). Collectively, these findings suggest that GPLD1 facilitates the selective lysosomal degradation of aberrant protein complexes through an HS-dependent mechanism at the cell surface (Fig. 6B).

SAA family proteins, including SAA1, are known to be upregulated in chronic inflammatory conditions such as metabolic syndrome, diabetes, and rheumatoid arthritis (Wilson *et al*, 2018). Elevated SAA1 expression has also been reported in the livers of patients with non-alcoholic fatty liver disease (Jiang *et al*, 2022). Similarly, GPLD1 expression is significantly increased in individuals with obesity, diabetes, and non-alcoholic fatty liver disease (Cao *et al.*, 2023). Considering the lysosomal uptake activity of GPLD1 demonstrated in this study, it is plausible that GPLD1 is upregulated to facilitate the degradation of elevated SAA1 during inflammatory responses. Although this study focused on amyloidosis-associated proteins to identify GPLD1, our findings show that GPLD1 is also effective in targeting misfolded proteins beyond amyloidogenic substrates. Therefore, GPLD1 may have potential therapeutic applications across a broad spectrum of protein misfolding-related diseases.

A comparison of substrate selectivity between GPLD1 and clusterin revealed that GPLD1 exhibits higher uptake activity for SAA1 than clusterin (Fig. 6A), suggesting that SAA1 is a specific substrate of GPLD1. GPLD1 is primarily secreted by the liver and is present in the bloodstream at relatively high concentrations (approximately 40-160 μg/ml) (Bjelosevic *et al*, 2017; Qin *et al*, 2016). This high level may reflect its role in rapidly clearing aberrant proteins that arise in circulation. Although the liver is the main source of GPLD1 secretion, it is also expressed in the brain (Cao *et al.*, 2023). The presence of GPLD1 in the brain suggests a potential role in the uptake of amyloidosis-associated proteins, which may help prevent Alzheimer's disease. Supporting this, increased GPLD1 expression has been reported to reduce Aβ42 levels through interactions involving Galectin-3 binding protein (Seki *et al*, 2020), indicating an indirect connection between GPLD1 and amyloid pathology.

We investigated whether HS, known to serve as a cell surface receptor for clusterin, also plays a role in GPLD1 internalization. In EXT1 KO cells, which lack HS chains (McCormick *et al.*, 1998), substrate-dependent uptake of GPLD1 was significantly reduced (Fig. 5B). Additionally, the presence of heparin in the culture medium, which mimics HS chains, decreased GPLD1 internalization (Fig. 5C). However, internalization was not completely abolished in EXT1 KO cells (Fig. 5B), indicating that although HS chains are not essential receptors, they likely facilitate GPLD1

uptake at the cell surface. It is plausible that HS chains, due to their extended polysaccharide structure, tether extracellular GPLD1 and may transfer it to an as-yet unidentified cell surface receptor. Indeed, HS chains function as receptors for fibroblast growth factor 2 (FGF2), enhancing its binding to the FGF2 receptor (Nadanaka & Kitagawa, 2018; Xu & Esko, 2014). Although the GPLD1-substrate complex is selectively internalized upon substrate binding, the mechanism by which endocytosis is preferentially promoted for this complex rather than GPLD1 alone remains unclear. We propose that binding of aberrant proteins induces a conformational change in GPLD1, enabling interaction with an unknown cell surface receptor that mediates internalization. Future studies aimed at identifying this receptor will be crucial to fully understand GPLD1-mediated uptake.

GPLD1 exhibits enzymatic activity that cleaves the lipid-binding site of GPI-anchored proteins exposed on the cell surface, thereby releasing them from the membrane (Cao *et al.*, 2023). These released GPI-anchored proteins are thought to influence chronic diseases by modulating various metabolic pathways (Cao *et al.*, 2023). To explore the relationship between GPLD1's enzymatic activity and its internalization, we generated catalytic mutants and conducted internalization assays. The GPLD1 H133N and H158N mutants, which display nearly undetectable enzymatic activity in biochemical assays (Raikwar *et al.*, 2005), retained their ability to undergo internalization (Fig. 4A), indicating that enzymatic activity is not essential for this process. Additionally, internalization assays using cells deficient in GPI-anchored proteins confirmed that GPLD1 internalization occurs independently of these proteins (Fig. 4B). Notably, GPLD1's enzymatic function has been shown to be required for cognitive improvements in mice (Horowitz *et al.*, 2020). Thus, GPLD1 appears to be a bifunctional molecule, both cleaving GPI-anchored proteins and facilitating the degradation of aberrant proteins. Given that the accumulation of aberrant proteins is linked to impaired brain function (Currais *et al*, 2017), GPLD1 may contribute to neural health through a synergistic mechanism involving both its enzymatic activity and its role in aberrant protein internalization.

Molecular chaperones were originally defined as factors that assist in protein folding. Conversely, extracellular chaperones function primarily to maintain the solubility of abnormal proteins by binding them directly and preventing aggregation in the extracellular environment (Wyatt *et al.*, 2013). Given the low ATP concentration outside the cell, extracellular chaperones lack refolding activity. Indeed, extracellular chaperones such as clusterin do not possess ATPase domains (Poon *et al*, 2000) but effectively inhibit stress-induced protein aggregation (Humphreys *et al*, 1999). Whether GPLD1 can similarly prevent aggregate formation remains to be determined. Based on current evidence, GPLD1 functions as a scavenger chaperone that facilitates the lysosomal degradation of aberrant proteins in the extracellular space. It exhibits distinct substrate selectivity from clusterin and operates within the CRED pathway (Fig. 6B). Further investigation is needed to elucidate the molecular mechanisms underlying GPLD1-mediated degradation of extracellular aberrant proteins, which may inform novel therapeutic strategies for their removal. Recently, several lysosome-targeting chimeras (LYTACs) have been developed to artificially degrade extracellular substrates by employing bifunctional molecules that bind both the plasma membrane and the target protein (Banik *et al*, 2020; Kim *et al*, 2024). However, because these chimeras are transported to

lysosomes even in the absence of substrate, repeated dosing may be required over time. Conversely, administration of scavenger chaperones such as GPLD1 and clusterin may prove more efficient, as substrate binding triggers their lysosomal transport. Therefore, a thorough understanding of the substrate recognition mechanism of GPLD1 is critical to effectively target specific extracellular substrates. Collectively, our findings provide valuable insights into extracellular proteostasis and advance the field of selective degradation of extracellular aberrant proteins.

Methods

Cell culture

Flp-In T-Rex HEK293 cells (Thermo Fisher Scientific, Waltham, MA, USA; cat# R78007), HepG2 cells (RIKEN BRC, cat# RCB1648), and U2OS cells were cultured in Dulbecco's modified Eagle medium (DMEM; Nacalai Tesque). T98G cells (JCRB, cat# IFO50303) were maintained in Eagle's minimum essential medium (MEM; Nacalai Tesque). HuEhT-2 cells (JCRB, cat# JCRB1459) were cultured in MCDB131 medium (Thermo Fisher Scientific) supplemented with 0.03 g/L endothelial cell growth supplement (ECGS), 5 µg/mL heparin, and 10 mM L-glutamine. All media were further supplemented with 10% fetal bovine serum (FBS; Biosera) and 50 µg/mL penicillin-streptomycin. Cells were maintained in a humidified incubator at 37°C with 5% CO_2. To generate stable cell lines with doxycycline-inducible expression of secreted proteins (e.g., GPLD1-mCherry-sfGFP-His), Flp-In T-Rex HEK293 cells were co-transfected with plasmids encoding the proteins of interest and pOG44, which encodes FLP recombinase. Transfected cells were selected and maintained in medium containing 100 µg/mL hygromycin. Gene expression at the FRT site was induced by treatment with 200 ng/mL doxycycline (Clontech).

Plasmids

To construct GPLD1-mCherry-sfGFP-His (GPLD1-RG) and GPLD1-Gamillus-His (GPLD1-Gamillus), full-length human GPLD1 was amplified from total cDNA extracted from HepG2 cells by PCR. Gamillus was amplified from pcDNA3-Gamillus (a gift from Dr. Takeharu Nagai, Osaka University) (Shinoda *et al.*, 2018). The amplified cDNAs were cloned into the pcDNA5 FRT TO vector along with sequences encoding mCherry, sfGFP, Gamillus, and a His-tag to generate pcDNA5 FRT TO GPLD1-RG and GPLD1-Gamillus constructs. GPLD1 mutants (H133N, H158N) were generated via site-directed mutagenesis. The pcDNA5 FRT TO clusterin-mCherry-sfGFP-His (clusterin-RG) construct was described previously (Itakura *et al.*, 2020). The pOG44 plasmid was used for the Flp-In recombination system. For the generation of His-ALFA-SAA1 and Ab42 (amyloid β1-42)-ALFA-His, SAA1 and Ab42 sequences were synthesized as gBlock Gene Fragments (Integrated DNA Technologies, Coralville, IA, USA). These fragments were inserted into the pRSET-A vector along with ALFA-tag and His-tag sequences to produce pRSET-A His-ALFA-SAA1 and pRSET-A Ab42-ALFA-His. To construct pCW SS-RFP-GFP-GPI, the signal sequence of prolactin, mCherry, sfGFP, and a 78-bp GPI-anchor sequence derived from prion protein were subcloned into the pCW57.1 vector (Addgene, cat# 41393). Lentiviral packaging plasmids pCMV-VSVG (Addgene, cat# 8454) and psPAX2 (Addgene, cat# 12260) were used for lentivirus production.

Generation of KO cells

EXT1 KO cells were generated as previously described (Itakura *et al.*, 2020). To create GPAA1 KO cells, a GPAA1-targeting sgRNA (CCTCTTACCGGTGGGTATTG) was cloned into lentiCRISPRv2 hygro (Addgene, cat#98291). HeLa cells were infected with lentivirus carrying Cas9 and the GPAA1 sgRNA. After 24 h, cells were selected with 100 µg/mL hygromycin for over 7 days, followed by

cloning via limiting dilution.

Antibodies

Rabbit polyclonal anti-LAMP1 antibody was kindly provided by Y. Tanaka (Kyushu University, Fukuoka, Japan). Rabbit polyclonal antibodies against sfGFP, mCherry, and the ALFA tag were generated by Eurofins using full-length mCherry protein and the ALFA peptide as antigens. Rabbit polyclonal anti-luciferase antibody (cat# PM016) was purchased from MBL. Rabbit polyclonal anti-β-actin (cat# 20536-1-AP) and anti-GPAA1 (cat# 10104-1-AP) antibodies were obtained from Proteintech. HRP-conjugated anti-rabbit antibody (cat# 7074S) was purchased from Cell Signaling Technology.

ALFA nanobody beads were prepared by conjugating ALFA nanobody protein (Götzke *et al*, 2019), purified from pRSET-A ALFA-His, to N-hydroxysuccinimide (NHS)-activated Sepharose 4 Fast Flow (GE). Similarly, GFP nanobody beads were prepared by conjugating GFP nanobody protein, purified from the pOPINE GFP nanobody plasmid (Addgene #49712), to NHS-activated Sepharose 4 Fast Flow (GE).

Recombinant proteins from *E. coli*

Recombinant luciferase was purchased from Promega (cat# E1701). His-ALFA-SAA1 and Ab42-ALFA-His were cloned into the pRSET-A vector and expressed in *E. coli* BL21(DE3) pLysS (Promega, cat# L1191). After harvesting, *E. coli* cells were disrupted by sonication. Following ultracentrifugation at 200,000 × *g* for 30 min at 4°C, the inclusion bodies (pellet fraction) containing His-ALFA-SAA1 or Ab42-ALFA-His were solubilized by sonication in urea buffer (8 M urea, PBS, 10 mM imidazole). To remove insoluble debris, the soluble fraction was subjected to ultracentrifugation at 200,000 × *g* for 30 min at 4°C. The resulting supernatant was purified using Co-NTA affinity chromatography under denaturing conditions (8 M urea, PBS). After elution using 200 mM imidazole buffer, purified His-ALFA-SAA1 and Ab42-ALFA-His were stored in the presence of urea. His-ALFA-ESD was described previously (Tomihari *et al.*, 2023).

Recombinant proteins from mammalian cells

For secreted proteins from mammalian cells, pcDNA5 FRT TO plasmids encoding GPLD1-RG-His, GPLD1-Gamillus-His, and Clusterin-RG-His were integrated into the FLP site of the genome in Flp-In T-Rex293 cells to generate stable (Tet-on) cell lines. Purification of secreted proteins from conditioned medium was performed as previously described (Tomihari *et al.*, 2021). Briefly, cells were cultured for 4 days in serum-free Advanced DMEM/F12 medium (Thermo Fisher Scientific, cat# 12634010) supplemented with L-glutamine and 0.2 μg/mL doxycycline. The culture supernatant was collected and centrifuged at 3500 rpm for 10 min at 4°C to remove dead cells. Secreted proteins were purified from the conditioned medium using Ni-NTA affinity chromatography. After elution using 200 mM imidazole buffer, the purified proteins were stored in PBS containing 10% glycerol.

Internalization assay

Purified GPLD1-RG (0.2 μM) or clusterin-RG (0.2 μM) in serum-free Advanced DMEM/F12

medium or serum-free conditioned medium containing secreted GPLD1-RG was mixed with substrate proteins. The mixtures were incubated as follows: luciferase (0.2 μM) was heat-treated at 42°C for 30 min; His-ALFA-ESD (8 μM) was heat-treated at 50°C for 1 h; and His-ALFA-SAA1 (8 μM) and Ab42-ALFA-His (8 μM) were incubated at 37°C with shaking for 2 h. After incubation, protein aggregates were removed by centrifugation at 15,000 rpm for 5 min. Cells were then cultured with the resulting supernatant (serum-free medium containing extracellular chaperone-RG with or without substrate) at 37°C for 18 h. In specified experiments, 0.1 μM BafA (LC Laboratories) or 80 μg/mL heparin (Nacalai Tesque) was added together with the medium. Cells were subsequently analyzed by flow cytometry, immunoblotting, or immunostaining.

Flow cytometry

Cells were detached using trypsin and resuspended in a solution containing 5% newborn calf serum and 1 μg/mL 4′,6-diamidino-2-phenylindole (DAPI) in PBS. The cell suspension was then passed through a 70 μm cell strainer and collected into a 1.5 mL tube. The collected cells were analyzed by flow cytometry using a CytoFLEX S flow cytometer (Beckman Coulter) equipped with 375-nm (DAPI), 488-nm (sfGFP), and 561-nm (mCherry) lasers. Dead cells were identified by DAPI staining and excluded from the analysis. A total of 10,000 live cells were measured.

Immunostaining and fluorescence microscopy

HuEhT-2 cells cultured on coverslips were fixed at room temperature for 15 min with 3.7% formaldehyde in PBS. For immunostaining, the fixed cells were permeabilized for 5 min with 50 μg/mL digitonin in PBS. After blocking with 10% newborn calf serum in PBS for 30 min, the cells were incubated with the primary antibody for 1 h. Following three washes with PBS, cells were incubated for 1 h with Alexa Fluor 568-conjugated goat anti-rabbit IgG antibody (Thermo Fisher Scientific). The cells were then mounted with a DAPI/DABCO/Glycerol/PBS solution. Stained cells were observed using a confocal laser scanning microscope (FV1000IX81; Olympus, Tokyo, Japan) equipped with a 100× oil immersion lens (NA 1.40).

Cell lysis and immunoblotting

Cells were washed with cold PBS and lysed for 15 min at 4°C in lysis buffer containing 1% Triton X-100, 50 mM Tris-HCl (pH 7.5), 1 mM EDTA, and 150 mM NaCl, supplemented with an EDTA-free protease inhibitor cocktail (Nacalai Tesque) and 1 mM phenylmethanesulfonyl fluoride (PMSF). After centrifugation at 20,000 × *g* for 5 min, the supernatant was collected, mixed with 6× SDS sample buffer, and boiled at 95°C for 5 min. Proteins were separated by SDS-PAGE, transferred to a polyvinylidene difluoride membrane (Millipore, cat# IPVH00010), and probed with antibodies diluted in Signal Enhancer HIKARI (Nacalai Tesque, cat# 02270-81). Protein bands were visualized using ImmunoStar Zeta (Fujifilm Wako Pure Chemical Industries, cat# 297-72404).

Identification of SAA1-binding proteins

ALFA-SAA1 (8 μM) was added to 50% bovine plasma (Rockland Immunochemicals, cat# D500-06-0500) diluted in PBS and incubated for 16 h at 4°C. The plasma was then centrifuged at

20,000 × *g* for 10 min to remove debris. The supernatant was mixed with ALFA-nanobody beads and rotated for 1 h at 4°C. The beads were washed four times with PBS, transferred to a new tube, mixed with SDS sample buffer, and boiled for 5 min, followed by mass spectrometry analysis.

Immunoprecipitation

Purified GPLD1-RG (final concentration: 10 nM for GFP IP, 40 nM for ALFA IP) and substrate proteins (final concentration: 40 nM luciferase for GFP IP, 10 nM His-ALFA-SAA1 for ALFA IP) were mixed in PBS and incubated at 4°C, except luciferase which was incubated at 42°C for 30 min and His-ALFA-SAA1 at 37°C for 2 h. After incubation, excess protein aggregates were removed by centrifugation at 20,000 × *g* for 5 min. GFP nanobody or ALFA nanobody beads (5 µL bed volume) were added to the supernatant and incubated at 4°C for 2 h. The beads were washed four times with PBS, transferred to a new tube, mixed with SDS sample buffer, and boiled for 5 min.

For the pulldown assay using heparin beads, 30 nM GPLD1-RG or 30 nM RG was mixed with heparin beads (M&S TechnoSystems, cat# Super-HEP10) in 0.04% BSA/PBS, in the presence or absence of 80 µg/mL free heparin, and then rotated for 2 h at 4°C. The beads were washed four times with PBS, transferred to a new tube, mixed with SDS sample buffer, and boiled for 5 min.

Statistical analysis

Data were collected from at least three biological replicates ($n \geq 3$). One-way ANOVA with Dunnett's post hoc test was used for significance testing in Figs. 1D, 3A, and 5B. One-way ANOVA with Tukey's post hoc test was used for Figs. 3C and 4A. Welch's t-test was applied for Fig. 5C. A p-value < 0.05 was considered statistically significant. Significance levels are indicated as follows: $^{*}p < 0.05$, $^{**}p < 0.01$, $^{***}p < 0.005$, $^{****}p < 0.001$; ns, not significant.

Acknowledgments

This work was supported by JSPS KAKENHI (grant nos. 20H03249, 22H04634, 23H04932, 24K02018 to E.I.), the JST FOREST Program (grant no. JPMJFR204N to E.I.), and the Takeda Science Foundation (to E.I.). We thank Dr. Yoshitaka Tanaka (Kyushu University) for providing the anti-LAMP1 antibodies, Dr. Takeharu Nagai (Osaka University) for the pcDNA3 Gamillus plasmid, and Dr. Reiko Nakagawa (Laboratory for Cell-Free Protein Synthesis, RIKEN Center for Biosystems Dynamics Research) for conducting the mass spectrometry experiments.

Author contributions

Mizuki Tsuchiya: Formal analysis; Validation; Investigation; Visualization; Writing—original draf. **Akira Matsuura**: Validation; Writing—original draft; Writing—review and editing. **Eisuke Itakura**: Conceptualization; Formal analysis; Supervision; Investigation; Visualization; Funding acquisition; Writing—original draft; Project administration; Writing—review and editing

Competing interests

The authors declare no conflicts of interest.

References

Banik SM, Pedram K, Wisnovsky S, Ahn G, Riley NM, Bertozzi CR (2020) Lysosome-targeting chimaeras for degradation of extracellular proteins. *Nature* 584: 291-297

Baravalle G, Schober D, Huber M, Bayer N, Murphy RF, Fuchs R (2005) Transferrin recycling and dextran transport to lysosomes is differentially affected by bafilomycin, nocodazole, and low temperature. *Cell Tissue Res* 320: 99-113

Bjelosevic S, Pascovici D, Ping H, Karlaftis V, Zaw T, Song X, Molloy MP, Monagle P, Ignjatovic V (2017) Quantitative Age-specific Variability of Plasma Proteins in Healthy Neonates, Children and Adults. *Mol Cell Proteomics* 16: 924-935

Calero M, Rostagno A, Matsubara E, Zlokovic B, Frangione B, Ghiso J (2000) Apolipoprotein J (clusterin) and Alzheimer's disease. *Microsc Res Tech* 50: 305-315

Cao J, Zhou A, Zhou Z, Liu H, Jia S (2023) The role of GPLD1 in chronic diseases. *J Cell Physiol* 238: 1407-1415

Currais A, Fischer W, Maher P, Schubert D (2017) Intraneuronal protein aggregation as a trigger for inflammation and neurodegeneration in the aging brain. *FASEB J* 31: 5-10

Eisenhaber B, Eisenhaber S, Kwang TY, Grüber G, Eisenhaber F (2014) Transamidase subunit GAA1/GPAA1 is a M28 family metallo-peptide-synthetase that catalyzes the peptide bond formation between the substrate protein's omega-site and the GPI lipid anchor's phosphoethanolamine. *Cell Cycle* 13: 1912-1917

Ellis RJ (2001) Macromolecular crowding: an important but neglected aspect of the intracellular environment. *Curr Opin Struct Biol* 11: 114-119

Gaffney PM (2017) Amyloid A Amyloidosis. *Vet Pathol* 54: 5-8

Glover JR, Lindquist S (1998) Hsp104, Hsp70, and Hsp40: a novel chaperone system that rescues previously aggregated proteins. *Cell* 94: 73-82

Götzke H, Kilisch M, Martínez-Carranza M, Sograte-Idrissi S, Rajavel A, Schlichthaerle T, Engels N, Jungmann R, Stenmark P, Opazo F *et al* (2019) The ALFA-tag is a highly versatile tool for nanobody-based bioscience applications. *Nat Commun* 10: 4403

Hipp MS, Kasturi P, Hartl FU (2019) The proteostasis network and its decline in ageing. *Nat Rev Mol Cell Biol* 20: 421-435

Horowitz AM, Fan X, Bieri G, Smith LK, Sanchez-Diaz CI, Schroer AB, Gontier G, Casaletto KB, Kramer JH, Williams KE *et al* (2020) Blood factors transfer beneficial effects of exercise on neurogenesis and cognition to the aged brain. *Science* 369: 167-173

Humphreys DT, Carver JA, Easterbrook-Smith SB, Wilson MR (1999) Clusterin has chaperone-like activity similar to that of small heat shock proteins. *J Biol Chem* 274: 6875-6881

517 Itakura E, Chiba M, Murata T, Matsuura A (2020) Heparan sulfate is a clearance receptor
518 for aberrant extracellular proteins. *J Cell Biol* 219
519 Jiang B, Wang D, Hu Y, Li W, Liu F, Zhu X, Li X, Zhang H, Bai H, Yang Q *et al* (2022) Serum
520 amyloid A1 exacerbates hepatic steatosis via TLR4-mediated NF-κB signaling pathway. *Mol*
521 *Metab* 59: 101462
522 Kim J, Byun I, Kim DY, Joh H, Kim HJ, Lee MJ (2024) Targeted protein degradation directly
523 engaging lysosomes or proteasomes. *Chem Soc Rev* 53: 3253-3272
524 Klionsky DJ, Petroni G, Amaravadi RK, Baehrecke EH, Ballabio A, Boya P, Bravo-San Pedro
525 JM, Cadwell K, Cecconi F, Choi AMK *et al* (2021) Autophagy in major human diseases. *EMBO*
526 *J* 40: e108863
527 LeBoeuf RC, Caldwell M, Guo Y, Metz C, Davitz MA, Olson LK, Deeg MA (1998) Mouse
528 glycosylphosphatidylinositol-specific phospholipase D (Gpld1) characterization. *Mamm*
529 *Genome* 9: 710-714
530 Liu J, Thorp SC (2002) Cell surface heparan sulfate and its roles in assisting viral
531 infections. *Med Res Rev* 22: 1-25
532 Louros N, Schymkowitz J, Rousseau F (2023) Mechanisms and pathology of protein misfolding
533 and aggregation. *Nat Rev Mol Cell Biol* 24: 912-933
534 Mahley RW, Weisgraber KH, Huang Y (2009) Apolipoprotein E: structure determines function,
535 from atherosclerosis to Alzheimer's disease to AIDS. *J Lipid Res* 50 Suppl: S183-188
536 Matsubara E, Soto C, Governale S, Frangione B, Ghiso J (1996) Apolipoprotein J and
537 Alzheimer's amyloid beta solubility. *Biochem J* 316 (Pt 2): 671-679
538 McCormick C, Leduc Y, Martindale D, Mattison K, Esford LE, Dyer AP, Tufaro F (1998) The
539 putative tumour suppressor EXT1 alters the expression of cell-surface heparan sulfate.
540 *Nat Genet* 19: 158-161
541 Nadanaka S, Kitagawa H (2018) Exostosin-like 2 regulates FGF2 signaling by controlling
542 the endocytosis of FGF2. *Biochim Biophys Acta Gen Subj* 1862: 791-799
543 Pillay S, Meyer NL, Puschnik AS, Davulcu O, Diep J, Ishikawa Y, Jae LT, Wosen JE, Nagamine
544 CM, Chapman MS *et al* (2016) An essential receptor for adeno-associated virus infection.
545 *Nature* 530: 108-112
546 Poon S, Easterbrook-Smith SB, Rybchyn MS, Carver JA, Wilson MR (2000) Clusterin is an
547 ATP-independent chaperone with very broad substrate specificity that stabilizes stressed
548 proteins in a folding-competent state. *Biochemistry* 39: 15953-15960
549 Qin W, Liang YZ, Qin BY, Zhang JL, Xia N (2016) The Clinical Significance of Glycoprotein
550 Phospholipase D Levels in Distinguishing Early Stage Latent Autoimmune Diabetes in Adults
551 and Type 2 Diabetes. *PLoS One* 11: e0156959

552 Raikwar NS, Bowen RF, Deeg MA (2005) Mutating His29, His125, His133 or His158 abolishes
553 glycosylphosphatidylinositol-specific phospholipase D catalytic activity. *Biochem J* 391:
554 285-289
555 Ren T, He J, Zhang T, Niu A, Yuan Y, Zuo Y, Miao Y, Zhang H, Zang L, Qiao C *et al* (2024)
556 Exercise activates interferon response of the liver via Gpld1 to enhance antiviral innate
557 immunity. *Sci Adv* 10: eadk5011
558 Rodrigo-Brenni MC, Gutierrez E, Hegde RS (2014) Cytosolic quality control of mislocalized
559 proteins requires RNF126 recruitment to Bag6. *Mol Cell* 55: 227-237
560 Rusilowicz-Jones EV, Urbé S, Clague MJ (2022) Protein degradation on the global scale.
561 *Mol Cell* 82: 1414-1423
562 Sawaya MR, Hughes MP, Rodriguez JA, Riek R, Eisenberg DS (2021) The expanding amyloid
563 family: Structure, stability, function, and pathogenesis. *Cell* 184: 4857-4873
564 Seki T, Kanagawa M, Kobayashi K, Kowa H, Yahata N, Maruyama K, Iwata N, Inoue H, Toda T
565 (2020) Galectin 3-binding protein suppresses amyloid-β production by modulating
566 β-cleavage of amyloid precursor protein. *J Biol Chem* 295: 3678-3691
567 Shinoda H, Ma Y, Nakashima R, Sakurai K, Matsuda T, Nagai T (2018) Acid-Tolerant Monomeric
568 GFP from Olindias formosa. *Cell Chem Biol* 25: 330-338.e337
569 Sipe JD, Benson MD, Buxbaum JN, Ikeda SI, Merlini G, Saraiva MJ, Westermark P (2016) Amyloid
570 fibril proteins and amyloidosis: chemical identification and clinical classification
571 International Society of Amyloidosis 2016 Nomenclature Guidelines. *Amyloid* 23: 209-213
572 Sun L, Ye RD (2016) Serum amyloid A1: Structure, function and gene polymorphism. *Gene* 583:
573 48-57
574 Tomihari A, Chiba M, Matsuura A, Itakura E (2021) Protocol for quantification of the
575 lysosomal degradation of extracellular proteins into mammalian cells. *STAR Protoc* 2:
576 100975
577 Tomihari A, Kiyota M, Matsuura A, Itakura E (2023) Alpha 2-macroglobulin acts as a clearance
578 factor in the lysosomal degradation of extracellular misfolded proteins. *Sci Rep* 13: 4680
579 Tyedmers J, Mogk A, Bukau B (2010) Cellular strategies for controlling protein aggregation.
580 *Nat Rev Mol Cell Biol* 11: 777-788
581 Uhlar CM, Whitehead AS (1999) Serum amyloid A, the major vertebrate acute-phase reactant.
582 *Eur J Biochem* 265: 501-523
583 Wilson PG, Thompson JC, Shridas P, McNamara PJ, de Beer MC, de Beer FC, Webb NR, Tannock
584 LR (2018) Serum Amyloid A Is an Exchangeable Apolipoprotein. *Arterioscler Thromb Vasc Biol*
585 38: 1890-1900
586 Wolff S, Weissman JS, Dillin A (2014) Differential scales of protein quality control. *Cell*
587 157: 52-64

588 Wyatt AR, Yerbury JJ, Ecroyd H, Wilson MR (2013) Extracellular chaperones and proteostasis.
589 *Annu Rev Biochem* 82: 295-322
590 Xu D, Esko JD (2014) Demystifying heparan sulfate-protein interactions. *Annu Rev Biochem*
591 83: 129-157
592 Yayon A, Klagsbrun M, Esko JD, Leder P, Ornitz DM (1991) Cell surface, heparin-like
593 molecules are required for binding of basic fibroblast growth factor to its high affinity
594 receptor. *Cell* 64: 841-848
595

Figure 1. Identification of GPLD1 as an extracellular scavenger chaperone

(**A**) Plasma proteins interact with SAA1. Bovine plasma was mixed with recombinant ALFA-SAA1, co-immunoprecipitated with ALFA nanobody beads, and analyzed by Ruby staining. Arrowheads indicate SAA1-binding proteins. (**B**) Schematic of the RFP-GFP internalization assay. Upon internalization, the protein of interest (POI) and GFP are degraded by lysosomal proteases, whereas RFP is resistant to lysosomal degradation and accumulates in lysosomes. (**C**) RFP intensity increases when GPLD1-RFP-GFP is incubated with SAA1. HEK293 cells were treated with serum-free medium containing POI-RFP-GFP with or without SAA1 for 18 h and analyzed by flow cytometry. (**D**, **E**) GPLD1-RFP-GFP is degraded in lysosomes. HEK293 cells were treated with serum-free medium containing GPLD1-RFP-GFP with or without ALFA-SAA1 in the presence or absence of bafilomycin A_1 (BafA) for 18 h. Cells were analyzed by flow cytometry (D) or immunoblotting using anti-mCherry and anti-β-tubulin antibodies (E). The bar graph shows relative fluorescence intensities normalized to non-treated cells (n = 3). Data are presented as mean ± SEM.

Figure 2. GPLD1 directly interacts with aberrant proteins

(**A**) Recombinant GPLD1-RFP-GFP was mixed with or without ALFA-SAA1 in PBS and preincubated at 37°C for 2 h. Samples were then subjected to immunoprecipitation using ALFA-nanobody beads at 4°C. (**B**) Recombinant GPLD1-RFP-GFP was mixed with or without luciferase in PBS and incubated at 42°C for 30 min. Samples were subjected to immunoprecipitation using GFP nanobody beads at 4°C.

Figure 3. GPLD1 mediates lysosomal degradation of misfolded proteins

(**A**) GPLD1-RFP-GFP internalization is enhanced in the presence of misfolded proteins. GPLD1-RFP-GFP was preincubated with luciferase (42°C for 30 min) or ALFA-ESD (50°C for 1 h) in serum-free medium. HEK293 cells were cultured with medium containing GPLD1-RFP-GFP with or without substrate for 18 h and analyzed by flow cytometry. The bar graph shows relative fluorescence intensities per cell normalized to untreated controls (n = 3). Data are presented as mean ± SEM. (**B**) GPLD1 is transported into lysosomes. HuEhT cells were treated with serum-free medium containing GPLD1-Gamillus, a lysosome-resistant GFP fusion, along with substrates. Cells were immunostained for LAMP1 (lysosomal marker) and imaged by confocal microscopy. Scale bar, 10 µm. (**C**, **D**) GPLD1-RFP-GFP and substrate complexes are degraded in lysosomes. HEK293 cells were treated as in (**A**) in the presence or absence of bafilomycin A_1, then analyzed by flow cytometry (C) or immunoblotting with anti-mCherry, anti-luciferase, and anti-β-tubulin antibodies (D).

Figure 4. GPLD1 internalization is independent of GPI-anchored protein cleavage

(**A**) Catalytic activity of GPLD1 is not required for its internalization. Wild-type (WT) GPLD1-RFP-GFP or catalytic mutants (H133N, H158N) were preincubated with luciferase (42°C for 30 min) or ALFA-SAA1 (37°C for 3 h) in serum-free medium. HEK293 cells were treated with medium containing GPLD1-RFP-GFP with or without substrate for 18 h and analyzed by flow cytometry. The bar graph shows relative fluorescence intensity per cell normalized to untreated controls (n = 3). Data are presented as mean ± SEM. (**B**) Confirmation of GPAA1 knockout (KO) by

immunoblotting wild-type and GPAA1 KO HeLa cell lysates with anti-GPAA1 antibody. (**C**) GPAA1 KO cells fail to mature GPI-anchored proteins. Wild-type and GPAA1 KO HeLa cells expressing GFP-GPI were analyzed by confocal microscopy. Scale bar, 10 μm. (**D**) GPLD1 internalization is not impaired in GPAA1 KO cells. Wild-type and GPAA1 KO HeLa cells were treated as in (A) and analyzed by flow cytometry.

Figure 5. Internalization of GPLD1 depends on heparan sulfate (HS)

(**A**) GPLD1 directly binds HS. Recombinant GPLD1-RFP-GFP or RFP-GFP, in the presence or absence of free heparin, was subjected to a pulldown assay using heparin-conjugated beads. (**B**) EXT1 KO cells show reduced GPLD1-RFP-GFP internalization. HEK293 wild-type (WT), EXT1 KO cells complemented with EXT1 (overexpression, OE), or empty vector were cultured in medium containing GPLD1-RFP-GFP as in Fig. 3A and analyzed by flow cytometry. The bar graph shows relative fluorescence intensity per cell normalized to untreated cells (n = 3). Data are presented as mean ± SEM. (**C**) Excess free heparin inhibits GPLD1-RFP-GFP internalization. GPLD1-RFP-GFP was incubated with luciferase (42°C for 30 min) or ALFA-ESD (50°C for 1 h) in serum-free medium. HEK293 cells (for luciferase) or HuEhT cells (for ALFA-ESD) were treated with medium containing GPLD1-RFP-GFP in the presence or absence of heparin for 18 h and analyzed by flow cytometry. The bar graph shows relative fluorescence intensity per cell normalized to the non-heparin treated control (n = 3). Data are presented as mean ± SEM.

Figure 6. GPLD1 and clusterin exhibit different specificities

(**A**) GPLD1, but not clusterin, shows higher specificity for SAA1. GPLD1-RFP-GFP (0.2 μM) or clusterin-RFP-GFP (0.2 μM) was incubated with luciferase (42°C for 30 min), ALFA-SAA (37°C for 3 h), or amyloid β1-42 (Ab42) (37°C for 3 h) in serum-free medium. HuEhT cells were treated with the medium containing GPLD1-RFP-GFP or clusterin-RFP-GFP, with or without substrate, for 18 h and analyzed by flow cytometry. The bar graph shows relative fluorescence intensity per cell normalized to non-treated controls (n = 3). Data are presented as mean ± SEM. (**B**) Model of the extracellular aberrant protein degradation pathway by GPLD1. GPLD1 interacts with misfolded proteins and SAA1, and the GPLD1 complex is delivered to lysosomes via cell surface heparan sulfate.

Figure S1. GPLD1-substrate complex is internalized in various cell lines

Various cell lines were treated with medium containing GPLD1-RFP-GFP as described in Figs. 1C and 3A and analyzed by flow cytometry.

Table S1. List of proteins identified by mass spectrometry.

The table shows the total spectral counts and the ratio of SAA1 to the control.

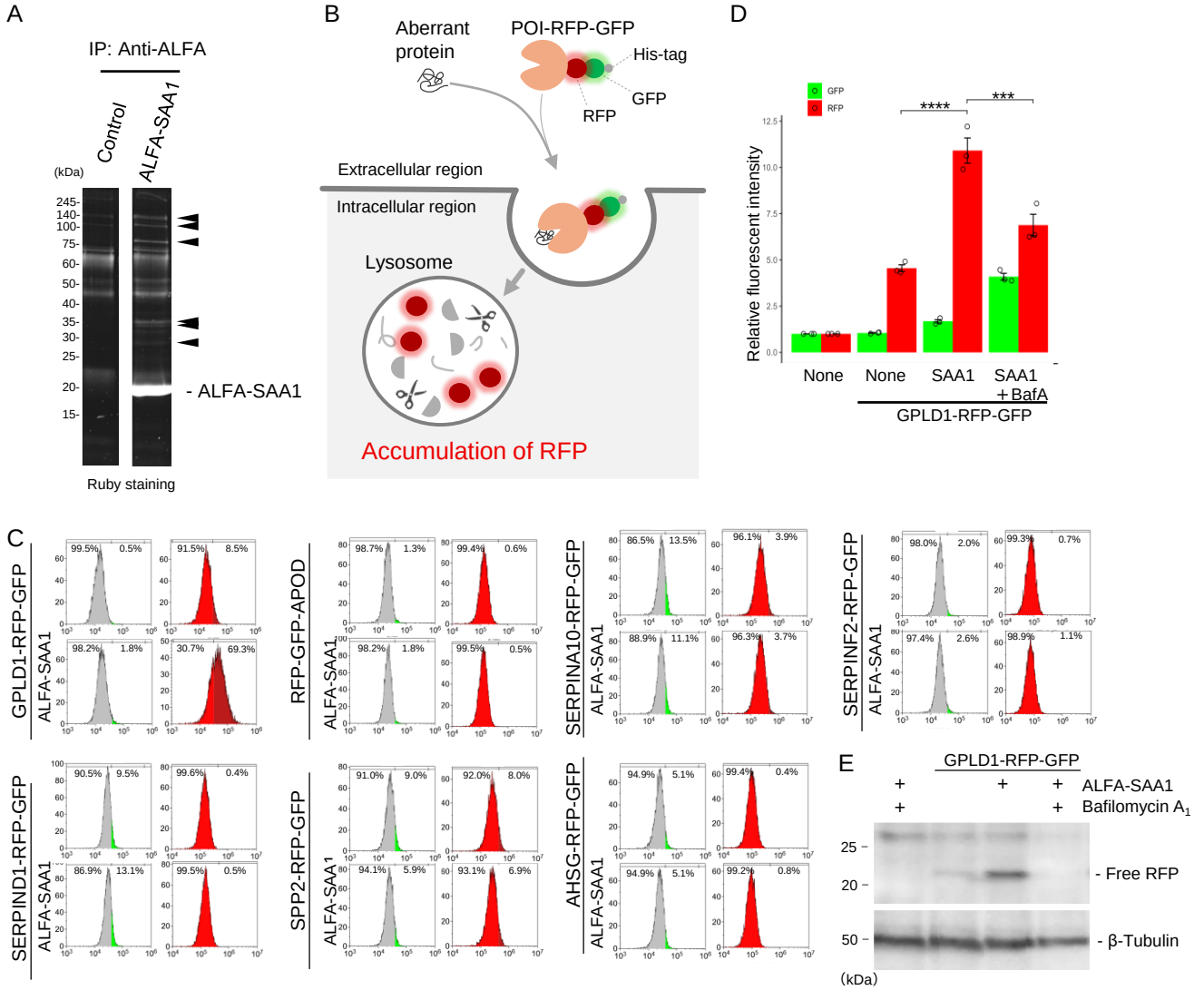

Figure 1. Identification of GPLD1 as an extracellular scavenger chaperone
(A) Plasma proteins interact with SAA1. Bovine plasma was mixed with recombinant ALFA-SAA1, co-immunoprecipitated with ALFA nanobody beads, and analyzed by Ruby staining. Arrowheads indicate SAA1-binding proteins. *(B)* Schematic of the RFP-GFP internalization assay. Upon internalization, the protein of interest (POI) and GFP are degraded by lysosomal proteases, whereas RFP is resistant to lysosomal degradation and accumulates in lysosomes. *(C)* RFP intensity increases when GPLD1-RFP-GFP is incubated with SAA1. HEK293 cells were treated with serum-free medium containing POI-RFP-GFP with or without SAA1 for 18 h and analyzed by flow cytometry. *(D, E)* GPLD1-RFP-GFP is degraded in lysosomes. HEK293 cells were treated with serum-free medium containing GPLD1-RFP-GFP with or without ALFA-SAA1 in the presence or absence of bafilomycin A_1 (BafA) for 18 h. Cells were analyzed by flow cytometry *(D)* or immunoblotting using anti-mCherry and anti-β-tubulin antibodies *(E)*. The bar graph shows relative fluorescence intensities normalized to non-treated cells (n = 3). Data are presented as mean ± SEM.

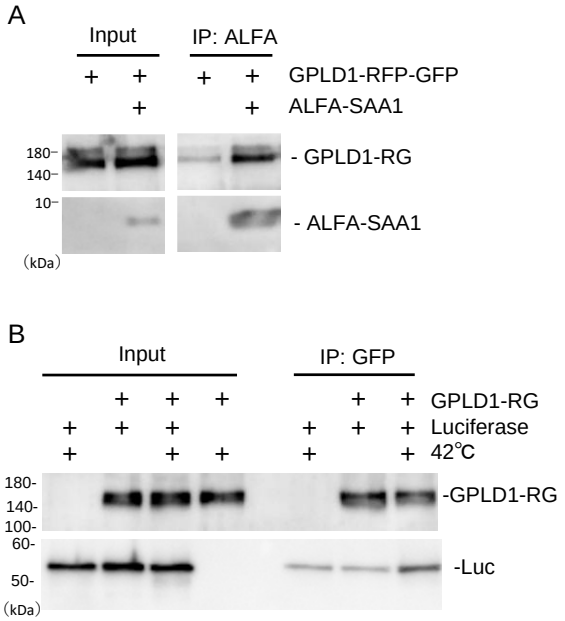

Figure 2. GPLD1 directly interacts with aberrant proteins
(A) Recombinant GPLD1-RFP-GFP was mixed with or without ALFA-SAA1 in PBS and preincubated at 37° C for 2 h. Samples were then subjected to immunoprecipitation using ALFA-nanobody beads at 4° C. *(B)* Recombinant GPLD1-RFP-GFP was mixed with or without luciferase in PBS and incubated at 42° C for 30 min. Samples were subjected to immunoprecipitation using GFP nanobody beads at 4° C.

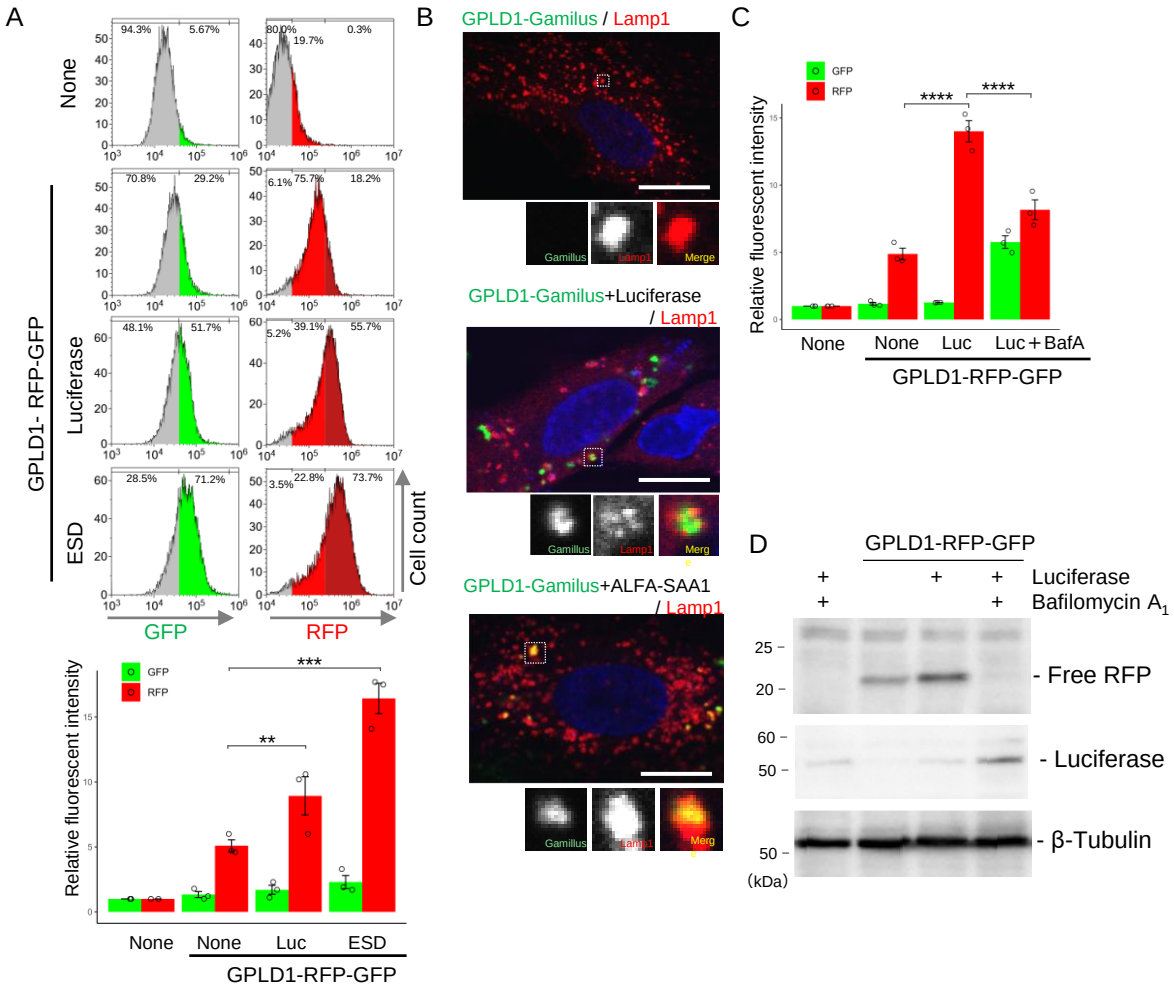

Figure 3. GPLD1 mediates lysosomal degradation of misfolded proteins
(A) GPLD1-RFP-GFP internalization is enhanced in the presence of misfolded proteins. GPLD1-RFP-GFP was preincubated with luciferase (42° C for 30 min) or ALFA-ESD (50° C for 1 h) in serum-free medium. HEK293 cells were cultured with medium containing GPLD1-RFP-GFP with or without substrate for 18 h and analyzed by flow cytometry. The bar graph shows relative fluorescence intensities per cell normalized to untreated controls (n = 3). Data are presented as mean ± SEM. *(B)* GPLD1 is transported into lysosomes. HuEhT cells were treated with serum-free medium containing GPLD1-Gamillus, a lysosome-resistant GFP fusion, along with substrates. Cells were immunostained for LAMP1 (lysosomal marker) and imaged by confocal microscopy. Scale bar, 10 µm. *(C, D)* GPLD1-RFP-GFP and substrate complexes are degraded in lysosomes. HEK293 cells were treated as in *(A)* in the presence or absence of bafilomycin A_1, then analyzed by flow cytometry *(C)* or immunoblotting with anti-mCherry, anti-luciferase, and anti-β-tubulin antibodies *(D)*.

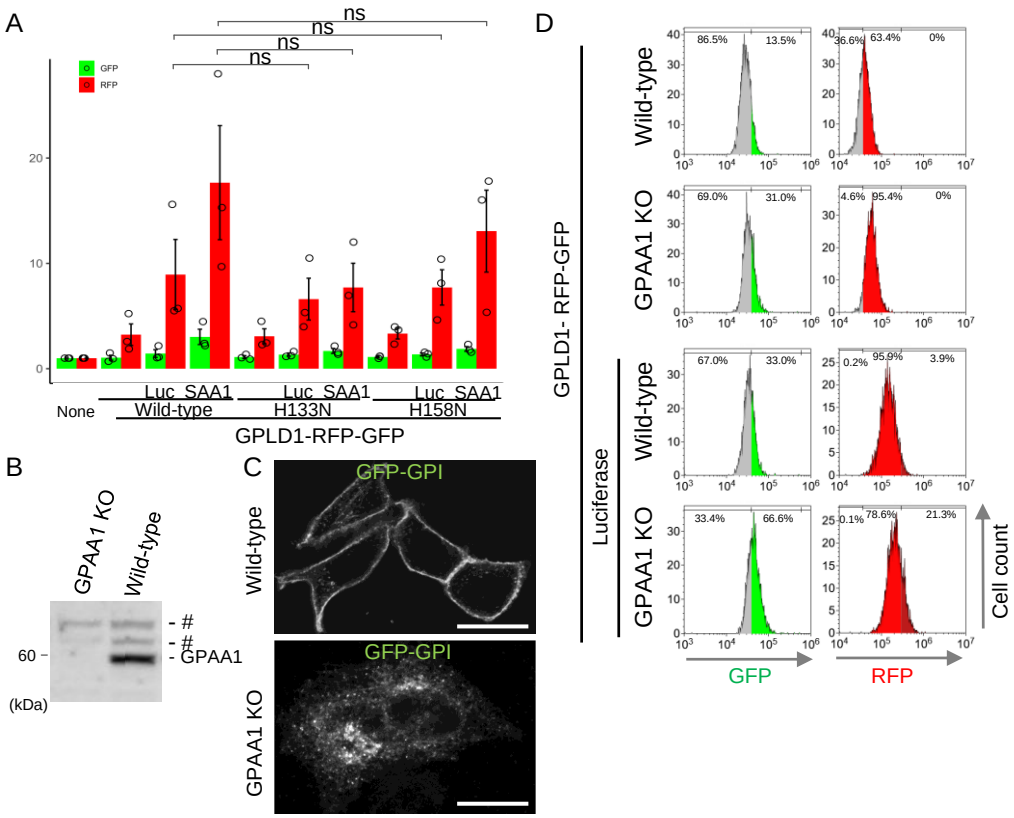

Figure 4. GPLD1 internalization is independent of GPI-anchored protein cleavage
(A) Catalytic activity of GPLD1 is not required for its internalization. Wild-type (WT) GPLD1-RFP-GFP or catalytic mutants (H133N, H158N) were preincubated with luciferase (42° C for 30 min) or ALFA-SAA1 (37° C for 3 h) in serum-free medium. HEK293 cells were treated with medium containing GPLD1-RFP-GFP with or without substrate for 18 h and analyzed by flow cytometry. The bar graph shows relative fluorescence intensity per cell normalized to untreated controls (n = 3). Data are presented as mean ± SEM. *(B)* Confirmation of GPAA1 knockout (KO) by immunoblotting wild-type and GPAA1 KO HeLa cell lysates with anti-GPAA1 antibody. *(C)* GPAA1 KO cells fail to mature GPI-anchored proteins. Wild-type and GPAA1 KO HeLa cells expressing GFP-GPI were analyzed by confocal microscopy. Scale bar, 10 µm. *(D)* GPLD1 internalization is not impaired in GPAA1 KO cells. Wild-type and GPAA1 KO HeLa cells were treated as in (A) and analyzed by flow cytometry.

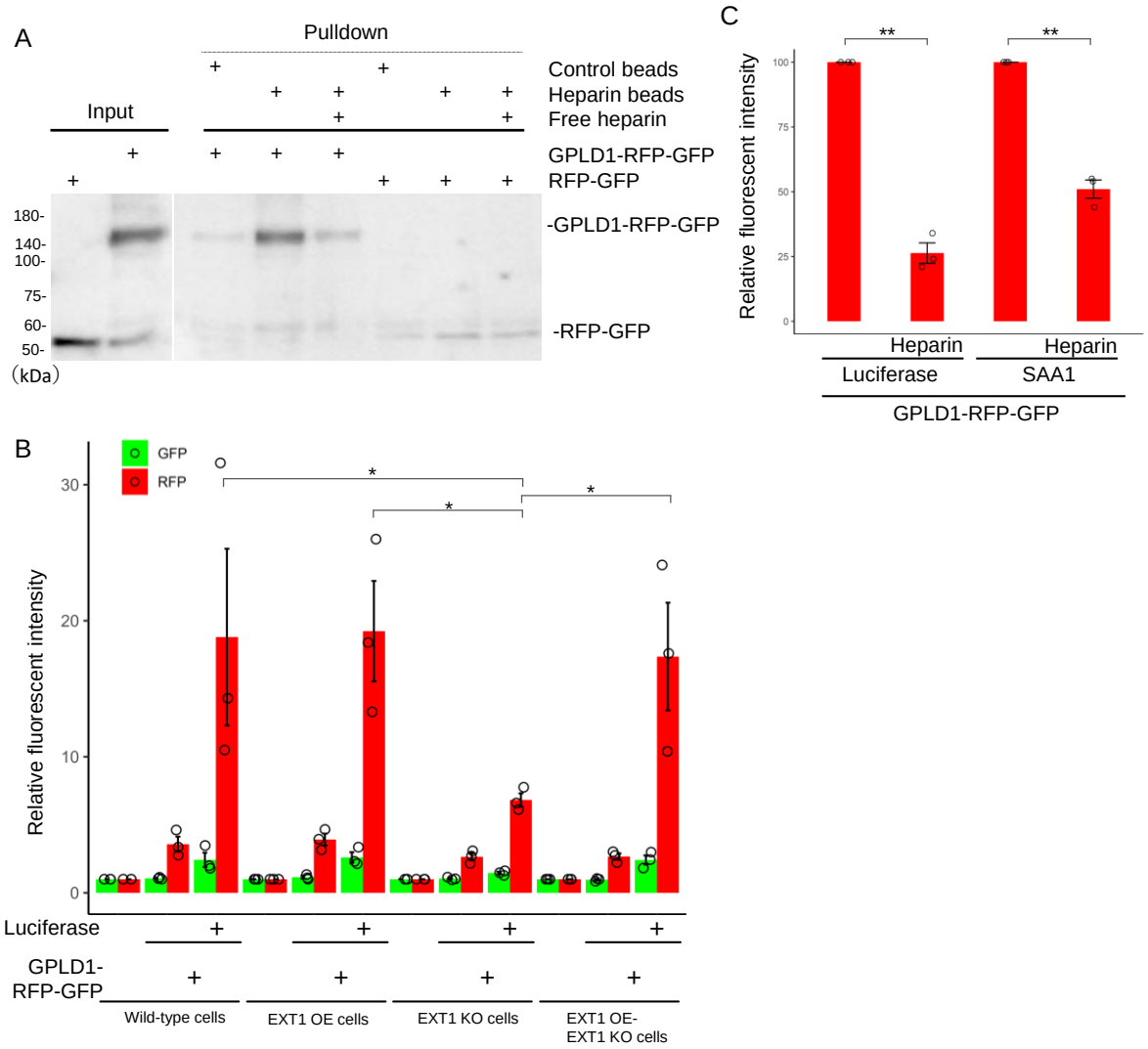

Figure 5. Internalization of GPLD1 depends on heparan sulfate (HS)
(A) GPLD1 directly binds HS. Recombinant GPLD1-RFP-GFP or RFP-GFP, in the presence or absence of free heparin, was subjected to a pulldown assay using heparin-conjugated beads. *(B)* EXT1 KO cells show reduced GPLD1-RFP-GFP internalization. HEK293 wild-type (WT), EXT1 KO cells complemented with EXT1 (overexpression, OE), or empty vector were cultured in medium containing GPLD1-RFP-GFP as in Fig. 3A and analyzed by flow cytometry. The bar graph shows relative fluorescence intensity per cell normalized to untreated cells (n = 3). Data are presented as mean ± SEM. *(C)* Excess free heparin inhibits GPLD1-RFP-GFP internalization. GPLD1-RFP-GFP was incubated with luciferase (42° C for 30 min) or ALFA-ESD (50° C for 1 h) in serum-free medium. HEK293 cells (for luciferase) or HuEhT cells (for ALFA-ESD) were treated with medium containing GPLD1-RFP-GFP in the presence or absence of heparin for 18 h and analyzed by flow cytometry. The bar graph shows relative fluorescence intensity per cell normalized to the non-heparin treated control (n = 3). Data are presented as mean ± SEM.

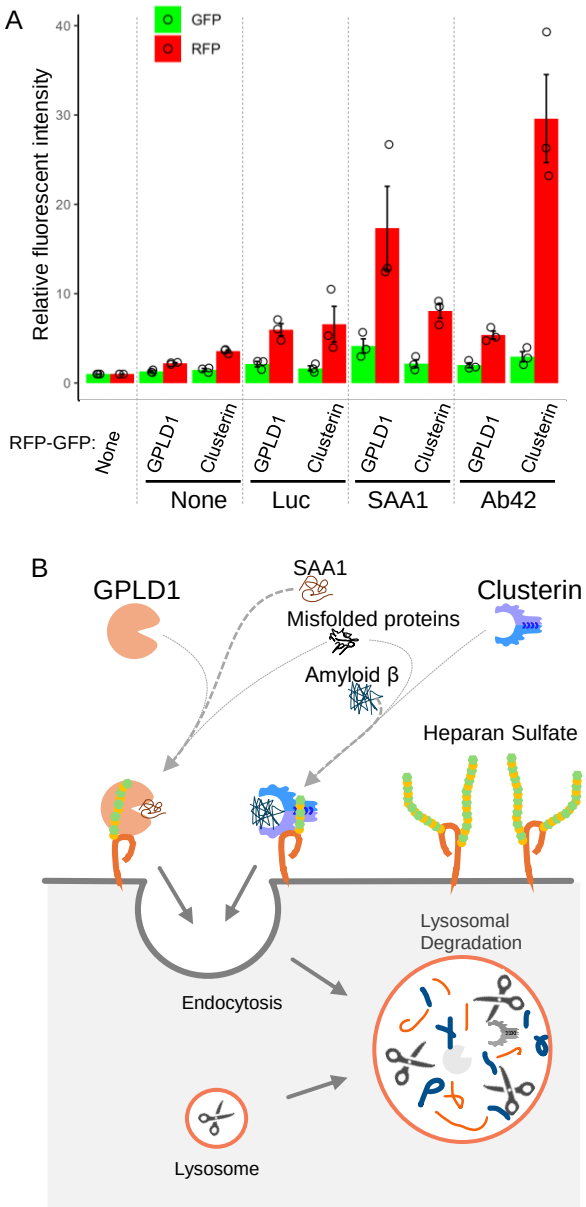

Figure 6. GPLD1 and clusterin exhibit different specificities
(A) GPLD1, but not clusterin, shows higher specificity for SAA1. GPLD1-RFP-GFP (0.2 μM) or clusterin-RFP-GFP (0.2 μM) was incubated with luciferase (42° C for 30 min), ALFA-SAA (37° C for 3 h), or amyloid β1-42 (Ab42) (37° C for 3 h) in serum-free medium. HuEhT cells were treated with the medium containing GPLD1-RFP-GFP or clusterin-RFP-GFP, with or without substrate, for 18 h and analyzed by flow cytometry. The bar graph shows relative fluorescence intensity per cell normalized to non-treated controls (n = 3). Data are presented as mean ± SEM. *(B)* Model of the extracellular aberrant protein degradation pathway by GPLD1. GPLD1 interacts with misfolded proteins and SAA1, and the GPLD1 complex is delivered to lysosomes via cell surface heparan sulfate.

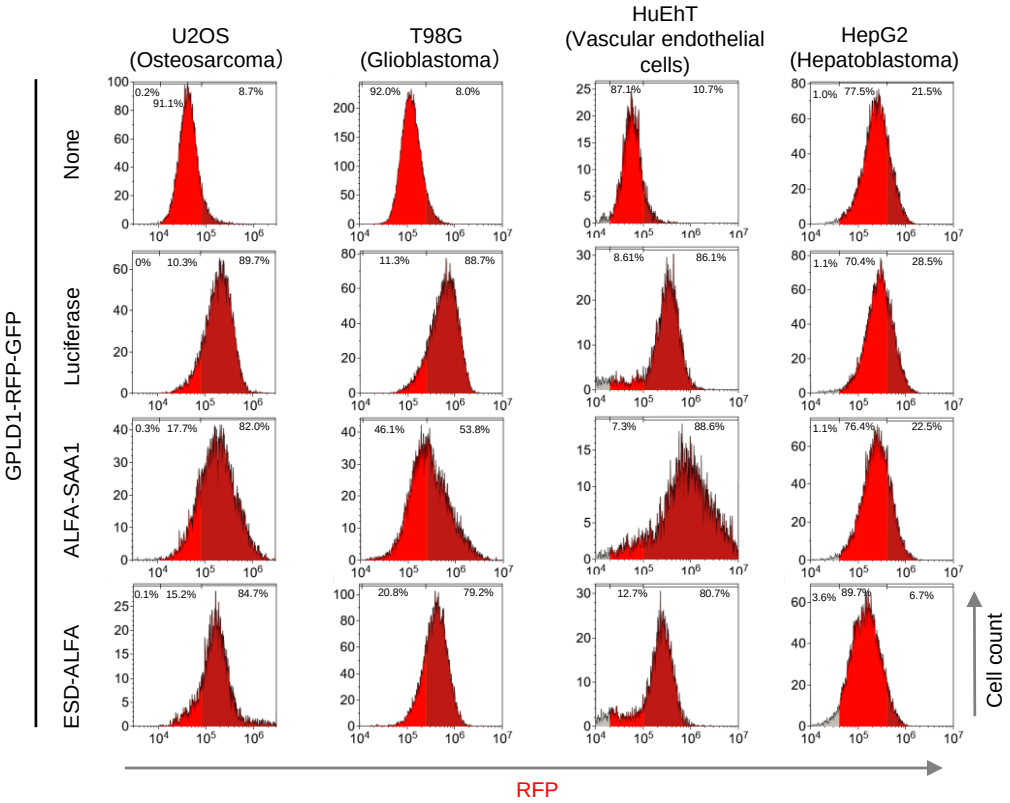

Figure S1. GPLD1-substrate complex is internalized in various cell lines
Various cell lines were treated with medium containing GPLD1-RFP-GFP as described in Figs. 1C and 3A and analyzed by flow cytometry.